VI International Conference on Computational Methods in Marine Engineering
MARINE 2015
F. Salvatore, R. Broglia and R. Muscari (Eds)

UNSTEADY LOADING ON THE PROPELLER AT DIFFERENT MANEUVERING CONDITIONS USING HYBRID AND URANS METHODS

NAWAR ABBAS*, NIKOLAI KORNEV†

*,†Chair of Modelling and Simulation,
University of Rostock,
A. Einstein Str., 2, 18059 Rostock, Germany
e-mails: nawar.abbas@uni-rostock.de, nikolai.kornev@uni-rostock.de,
web page: http://www.lemos.uni-rostock.de/en/

Key words: ship wake, propeller, URANS, LES, hybrid methods, manoeuvring, drift angle

Abstract. The results of computations of the unsteady wake and unsteady loadings on marine propellers behind the KVLCC2 tanker model under simple manoeuver conditions (only drift angle) and complete manoeuvring (drift angle and yaw rate) using different numerical methods are presented and analysed. The hybrid URANS-LES model presented in [1, 2], the hybrid IDDES and the k-ω-SST model are applied first for the bare hull at different drift angles, and then under complete manoeuvring conditions (different drift angles and yaw rates). The forces and moment coefficients of the bare hull calculations under different drift angels were compared with the experimental results of Kume et al. [3]. In the second series of calculations the arrangement containing both the ship and rotating propeller is computed with consideration of all interaction effects at different drift angles. Under complete manoeuvring condition the whole system (ship, rudder and propeller) was calculated using the hybrid method [1, 2]. CFD results for the time averaged thrust were compared with the experimental results [4]. Also the comparison for the standard deviations of forces and moments acting on propeller and its appendages with the experimental estimations is presented.

1 INTRODUCTION

In shipbuilding great attention is paid to the analysis of unsteady forces and moments, which act on ship during the manoeuvring and lead to vibrations of the hull structure particularly in the stern area where propeller is located. The unsteady loading on propeller is one of the most significant factors that causes the generation of such forces and moments. It is mainly produced by the inhomogeneity and velocity fluctuations in the

wake both caused by the boundary layer and concentrated vortex structures shed from the hull. During maneuvering, the effect of these factors increases which leads to increased turbulence behind the ship at the propeller disc. At these critical situations, a potential great rise in the level of thrust and torque fluctuations transmitted through the propeller shaft to ship hull might occur. Proper resolution of flow separations and vortex structures in ship flows at straight course and maneuvering conditions is the challenge for the Computational Fluid Dynamics (CFD). There are a lot of CFD computations for ships under different maneuver conditions which overview can be found in proceedings of the workshop SIMMAN-2008 devoted to the validation of the Ship Maneuvering Simulation Methods (see [5]). The performance of these methods were investigated for three types of ships: tankers, containers and surface combat (DTMB 4515). CFD results were compared with various experimental results obtained using different measurement methods including advanced stereo PIV (Stereo Particle Image Velocimetry) technique. Among different numerical simulations it is worth to mention the paper by Xing et al. [6] who used several numerical models like the blended $k-\varepsilon$/k-ω (BKW), DES (Detached Eddy Simulation), BKW-DES, Reynolds stress (RS) and RS-DES for numerical computations of the tanker model KVLCC2 at different drift angles 0°, 12° and 30° ignoring the effect of the free surface. The results confirm that the use of the RS model produces very good results for resistance coefficients, distribution of the axial velocity and the turbulent kinetic energy in the propeller plane. Calculations for the ship with the drift angle of 30 degrees reveal that the BKW & RS-RANS models give a steady solution while the RS-DES models is capable of reproducing unsteady effects. Computational experience shows that the URANS models alone are not able to capture all unsteady effects in ship flows. In order to capture these unsteady effects and instabilities it is necessary to use either pure LES models or hybrid URANS/LES methods. The most serious disadvantage of a pure LES approach is the necessity of a very high resolution close to the ship surface which is unrealistic for computer power available in shipbuilding research organizations. The problem can be overcome using special wall functions or, alternatively, the hybrid methods. To our opinion the hybrid URANS/LES approach is the most perspective way to handle the unsteady flows at high Reynolds numbers. Within this approach the near body flow region is treated using URANS and the far flow region is simulated with LES. Application of hybrid URANS/LES methods for ship flows was started in the last decade although the number of work is still restricted because of large computational resources needed for implementation of this approach.

2 OVERVIEW OF THE USED COMPUTATIONAL METHODS

Ship flow under maneuvering conditions is calculated in the ship fixed coordinate system. The linear and angular ship velocities are assumed to be constant. Fluid dynamic equations are rewritten in a moving frame of reference to take the Coriolis and centrifugal forces into account. The Reynolds turbulent stresses are calculated in this work using the κ-ω-SST model. Two kinds of hybrid approaches were utilized: the IDDES(Improved

Delayed Detached Eddy Simulation) proposed by Shur et al [7] and the hybrid approach developed at the Chair of Modeling and Simulation of the Rostock University [1, 2]. A brief summary of the latter method is explained in details in our previous works [1] and [2]. Also DMM (Dynamic Mixed Model) was used for the system containing both the ship and rotating propeller. All our CFD calculations were carried out with the OpenFOAM toolkit.

3 GEOMETRY AND THE NUMERICAL ENVIRONMENT

The doubled model of the KRISO tanker-KVLCC2 was selected for calculations because of large amount of experimental and numerical data available in the literature. The geometry of the models are shown in the Table. 1. We consider small Froude numbers ($Fn = 0.142$) and ignore the water surface deformations effects.

Table 1: Principal dimensions of the KVLCC2-model with the scale (1/64.4)=M_1, scale (1/58)=M_2 and scale (1/110)=M_3

Item	Symbol	Unit	M_1	M_2	M_3
Length between perpendiculars	L_{PP}	m	4.9700	5.5172	2.9091
Breadth (molded)	B	m	0.9008	1.0000	0.5273
Draft (molded)	d	m	0.3231	0.3586	0.1891
Wetted surface area without appendages	S_w	m^2	6.5597	8.0838	2.2475
Blockage coefficient	C_B	-	0.8098	0.8098	0.8098
Froude number	F_r	-	0.1420	0.1420	0.1420

The computation domain for all calculations is a box with dimensions L ×B ×T=4.61L ×2.88L ×1.51L. First, the calculations of the bare hull under different maneuvering conditions were performed for the M1 model using the grid with 13 million of cells. The grid has a sufficient refinement in the propeller disc, see Fig. 1(a). In our previous study [2] the influence of grid resolution on the velocity field fluctuations and vortex structures in the wake as well as the grid dependency of unsteady propeller loadings were presented. From this study one can conclude that 13 M cells grid is enough fine to capture most of important hydrodynamic effects in the nominal wake. The second part of the calculations are for the system M2 ship model with 5 blades rotating propeller VP1356. The propeller properties are $D = 0.170$ m, pitch ratio = 0.996, EAR = 0.8, $D_{hub}/D = 0.18$ and max. skewness = 33°. Numerical computations for this case were done under simple maneuvering conditions with different drift angles, 0°, 6°, 12°and 30°and propeller frequency $n = 9.35$ rps. The thrust of the propeller was equal to the ship resistance. We computed the rotating propeller using AMI-technique (Arbitrary Mesh Interface) to model the interface between stator and rotor grids. The system of the ship with the rotating propeller was studied using computational grid of 27 million of cells, the stator grid has been generated using Ansys ICEM software and contains 23 million of cells, the average value of y^+

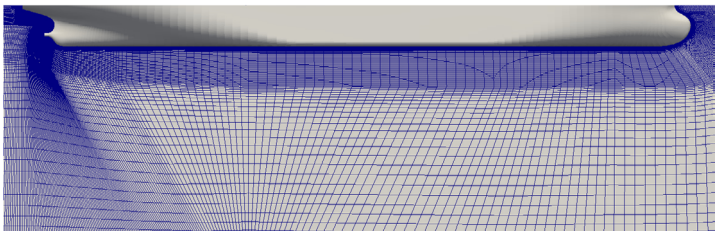

(a) Computational grid of KVLCC2.

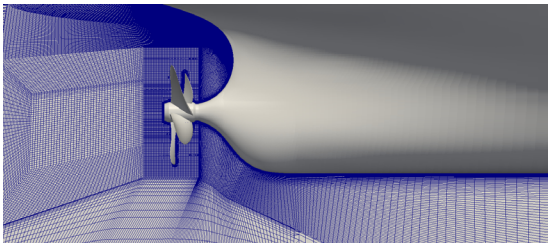

(b) Computational grid of KVLCC2 with propeller-VP1356.

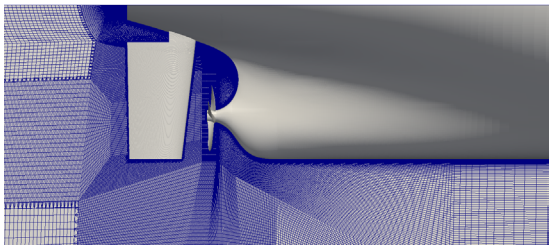

(c) Computational grid of KVLCC2 with propeller-MOERI and rudder.

Figure 1: Computational grid of KVLCC2 with appendages.

is 1.9. The rotor grid has been generated using the snappyHexMesh procedure available in openFOAM-software. The rotor grid contains 4 million of cells with the average value of $y^+ = 6.5$. The computational domain for the ship with rotating propeller is presented in Fig. 1(b). Computations were performed with Courant number between $25 - 35$ which corresponds to the time step of 5×10^{-4}s, thus the rotating angle of propeller for each time step is 1.683°. Finally, the whole system of the tanker-KVLCC2 with the scale 1/110 with propeller of four blades type MOERI and the rudder was calculated. The numerical computations for the whole system were performed under the following maneuvering conditions : *a1*: yaw rate $r = 0.2$ and drift angle β=6°; *a2*: r=0.2 and β=12°; *a3*: $r = 0.6$ and $\beta = 12°$. The computational domain for this case contains 30 million of cells. The startor grid for the hull and rudder was generated using Ansys ICEM software and contains 26 million of cells with the average value of y^+=0.6. After generating the stator hull grid the rudder was added using snappyHexMesh tool, the average value of y^+ at the first node from the rudder surface is equal to 3.8. The grid of the rotor domain (propeller) was generated using the snappyHexMesh as well and contains 4 million of cells with the average value of $y^+ = 7.0$. Fig. 1(c) illustrates the grid used in this study. As mentioned above, computations were performed using the OpenFOAM code. The spatial discretization of the convective term is performed using the filtered Linear scheme which calculates the face values using blending of linear interpolation with a particular amount of upwind, depending on the ratio of the background (in-cell) gradient and face gradient. The amount of upwind is limited to 20%. This way, the high-frequency oscillation modes are filtered out and thus the stable solution is obtained without a considerable increase of nu-

merical dissipation, which is undesirable for hybrid and LES simulations. Laplacian term was discretized using the linear scheme with explicit non-orthogonal correction. Pressure gradient was reconstructed using linear scheme based on the Green-Gauss theorem. The equations for k and ω were discretized in the same manner except the convective term, for which a TVD scheme with Sweby flux limiter was applied. The time discretization has been done using the Crank-Nicolson scheme. For the initialization of the flow in the computational domain the steady κ-ω-SST solution obtained using the simpleFoam solver has been utilized. After that the unsteady solver pisoFoam, which was modified to take the Coriolis and the centrifugal forces into account, was applied to get unsteady solution. Simulation time necessary to obtain averaged quantities corresponds to four ship lengths runs $4L_{PP}/U$ at least.

4 RESULTS FOR THE BARE HULL WITHOUT APPENDAGES

In what follows the designation "Hybrid" is used for numerical results obtained using the hybrid model [1, 2].

4.1 Integral hydrodynamic forces

The hydrodynamic forces are referred to the lateral area $d \cdot L_{pp}$. The coordinate system is given in Fig. 2a. Numerical results are compared with measurements performed in [3]. Since the experimental data at 0°, 9°, and 18° were averaged over eight sets of measurements for the uncertainty analysis purpose they deviate slightly from the curve obtained from single measurement. The symbol "I" (error bar) shows the data scattering. All data agree well with measurements. Results for all methods are approximately the same because the most part of the ship hull is in URANS mode which is treated well with both Spalart Allmares (in IDDES) and κ-ω-SST (in Hybrid) models.

4.2 Velocity field in the wake behind the bare hull without appendages

Analysis of the velocity field behind the bare hull at the propeller disc location is the first step in the study of thrust oscillations at straight course and maneuvering conditions. Within this subsection the results are presented only for the hybrid method [1, 2].

Fig. 3 shows the circumferential distribution of standard deviation at different radii and different maneuvering conditions. Obviously, when the drift angle and yaw rate increase, the standard deviation decrease for blade positions on the windward side at $0 < \Phi < 180$ degree. It is almost zero at the largest values of β and yaw rate for the whole radii range. On the contrary the turbulent fluctuations get larger on the leeward side at $180 < \Phi < 360$. The physics of this effect can relatively easy be explained. Due to asymmetric incident flow at $\beta \neq 0$ and $r \neq 0$ the wake is displaced towards the leeward side as shown in Fig. 6,e. As a result, the non-uniformity of the wake on the windward side is decreased, i.e. the flow on the port side becomes more uniform. On the contrary, both the non-uniformity and turbulence increase on the leeward side. Therefore, one can expect that

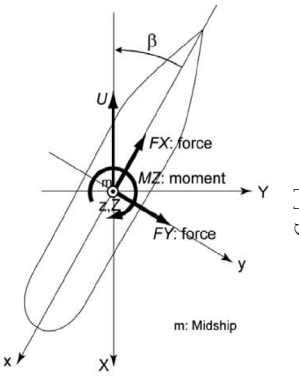

(a) Coordinate systems for hydrodynamic forces and moment [3].

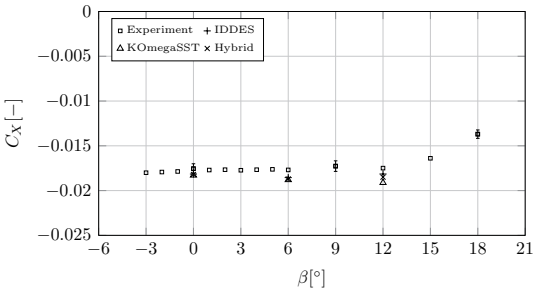

(b) Drag coefficient.

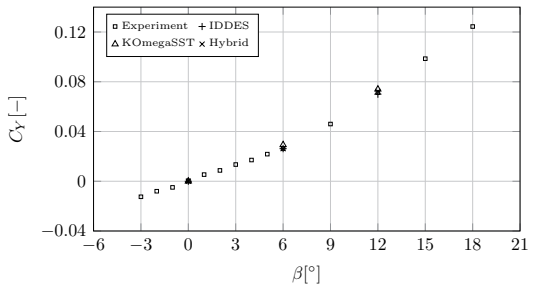

(c) Side force coefficient.

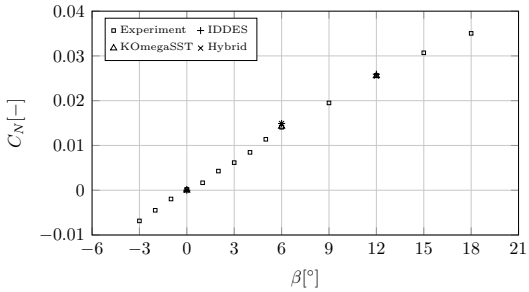

(d) Yaw moment coefficient.

Figure 2: Hydrodynamic force and moment coefficients versus drift angle β. Experimental data are taken from [3].

these effects result in the increase of the thrust fluctuations at maneuvering conditions. This increase is due to the two following reasons. First, the overall non-uniformity of the wake increases. Second, separation and vortex structures are strengthened at maneuvering conditions what leads to the increase of turbulent fluctuations.

5 UNSTEADY LOADINGS ON THE PROPELLER

5.1 Hull and propeller at drift angle without yaw

In our previous work [2], the results for the standard deviation of forces and moments acting on the propeller VP1356 while the ship sails straight forward were presented and discussed. Comparisons were made between the CFD results and the experimental estimation. CFD results in [2] were calculated using the Hybrid and κ-ω-SST methods, while the standard deviations based on engineering methods were calculated using amplitudes of different harmonics published in Bartrak et al 2012 [8]:

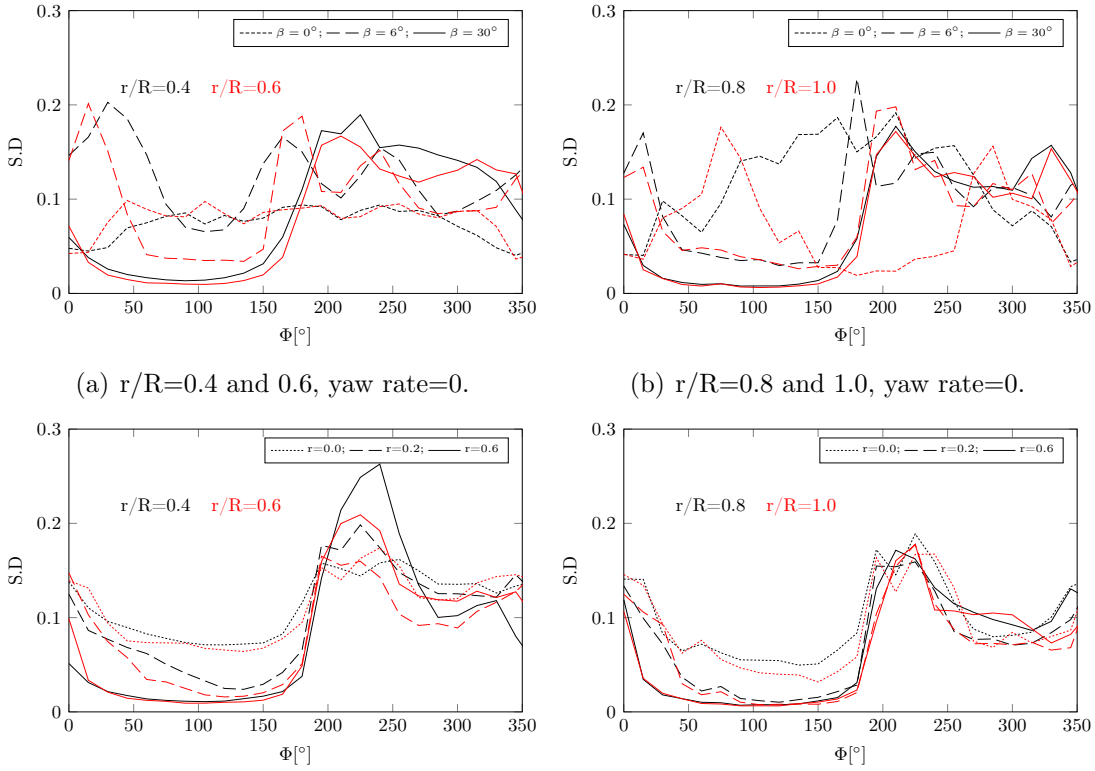

(a) r/R=0.4 and 0.6, yaw rate=0.

(b) r/R=0.8 and 1.0, yaw rate=0.

(c) r/R=0.4 and 0.6, β=12°.

(d) r/R=0.8 and 1.0, β=12°.

Figure 3: Standard deviation S.D. of axial velocity fluctuations along circles at different radii r/R in the propeller plane under different maneuvering conditions.

$$P'_x = (\overline{(P_x - \overline{P_x})^2})^{1/2} = \left[\lim_{T\to\infty} \frac{1}{T} \int_0^T \left(\sum_{k=1}^{N} A_k \sin(knZt + \phi_k) \right)^2 dt \right]^{1/2} \tag{1}$$

where A_k is the amplitude of $k-th$ mode, N is the number of harmonic modes (usually $N = 2$) and ϕ_k is the phase displacement. Amplitudes A_k are published in [8] for different blade numbers. Each amplitude is represented as the sum of a mean value which is valid for all possible ships and a deviation, i.e. $A_k = A_k^{mean} \pm A_k^{dev}$. A_k^{dev} accounts for the variation of A_k depending on ship types. Particularly, for full bottomed ships this reads $A_k^{max} = A_k^{mean} + A_k^{dev}$. Results obtained using A_k^{mean} are referred in Table 2 to as "mean". Since the phase displacement is not known, it is set to zero to get upper estimation for standard deviations. The same procedure is applied to all forces and moments. All force standard deviations are referred to the mean thrust, whereas the moments deviations to the mean torque.

Looking at results in Tab. 2, we can notice that the peaks of vertical and transversal

Table 2: Standard deviations of the forces and moments calculated using different approaches at different drift angels: V: Veritec, W: Wereldsma, S: Scheme B, H: Hybrid, KO: k-ω-SST and DMM: Dynamic Mixed Model. All force standard deviations are referred to the mean thrust, whereas the moments deviations to the mean torque. Other designations stand for: P_x: thrust, P_y: vertical force, P_z: horizontal force, M_x: torque, M_y: horizontal moment, M_z: vertical moment.

Methode	C-0°	W-0°	S.B-0°	0°	6°		12°			30°
	mean	mean	mean	H	H	H	KO	IDDES	DMM	H
$P'_x/\overline{P_x}\%$	1.85 ±0.47	2.47 ±1.41	1.77 ±1.13	0.88	2.61	3.16	1.43	5.34	8.03	3.88
$P'_y/\overline{P_x}\%$	0.79 ±0.65	1.96 ±1.41	0.19 ±0.15	0.29	0.73	1.27	0.60	1.67	1.97	0.97
$P'_z/\overline{P_x}\%$	1.54 ±1.16	2.32 ±1.41	0.74 ±0.44	0.51	0.95	1.43	0.84	1.63	1.80	1.16
$M'_x/\overline{M_x}\%$	0.12 ±0.55	1.76 ±1.41	1.34 ±0.75	0.74	1.90	2.26	1.00	4.00	6.31	3.00
$M'_y/\overline{M_x}\%$	10.15 ±6.84	6.41 ±1.41	1.63 ±1.23	1.94	3.17	4.50	2.65	8.25	9.86	3.36
$M'_z/\overline{M_x}\%$	10.49 ±6.61	3.74 ±1.41	5.17 ±3.03	2.31	3.79	5.61	3.90	7.12	8.76	5.35
$\overline{P_x}$	-	-	-	22.83	21.40	20.91	20.80	18.70	21.11	21.42

forces are approximately twice as small as these of the thrust. From the table above one can conclude that the value of the thrust standard deviation increases starting from 0.88 when β=0° up to 3.88 when β=30°. As for the forces in directions y and z, the standard deviation increases with the drift angle's increment until β=12° and then any change in its value (increment or decrement) becomes small. For example, the ratio $P'_y/\overline{P_x}\%$ changes within the $0.29-1.27$ range, whereas the force ratio $P'_z/\overline{P_x}\%$ changes within the $0.51-1.43$ range. The effect of the drift angle on time averaged value of the thrust is relatively weak. As for the standard deviation of the moments affecting the propeller, they increase when the drift angle gets larger until β=12° degrees, after that their change is rather small. Fig. 4 shows the variation of the thrust in time for each of κ-ω-SST, hybrid, IDDES and DMM simulations with a drift angle of β=12°degrees. As seen in Fig. 4, statistical convergence is attained at time $t > 10$ sek. The thrust predicted from URANS-κ-ω-SST model is strictly periodic and this seems to be totally unrealistic result considering that the ship sailing with a drift angle causes many instabilities in the wake which in turn have to lead to large chaotic thrust oscillations. Therefore, URANS method, which is widely used in the shipbuilding community, is not capable of modeling unsteady vortices arising in the ship stern area flow.

5.2 Hull, propeller and rudder with drift angle and yaw rate

Calculations were performed for the 4-blade MOERI propeller. Fig. 5 shows the time history of non-dimensional thrust $t\prime$ defined as $t\prime = T/(0.5\rho LdU^2)$, where T is the propeller thrust, under different maneuver conditions. Comparison was made between the CFD results using the Hybrid method and the time averaged experimental values.

Table 3 shows the standard deviations for the forces and moments acting on the 4-blade propeller for a ship moving straight forward, under different maneuver conditions as well as the experimental estimations for these deviations for a ship moving straight forward. Again, the forces are referred to the mean value of the thrust whereas the moments to the mean value of the torque M_x.

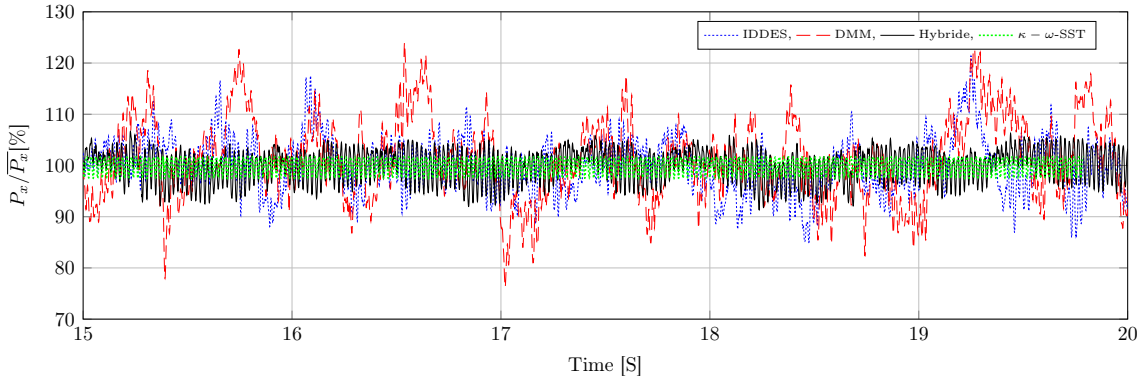

Figure 4: History of the thrust obtained by $\kappa-\omega$-SST, hybrid, DMM and IDDES models at β=12°.

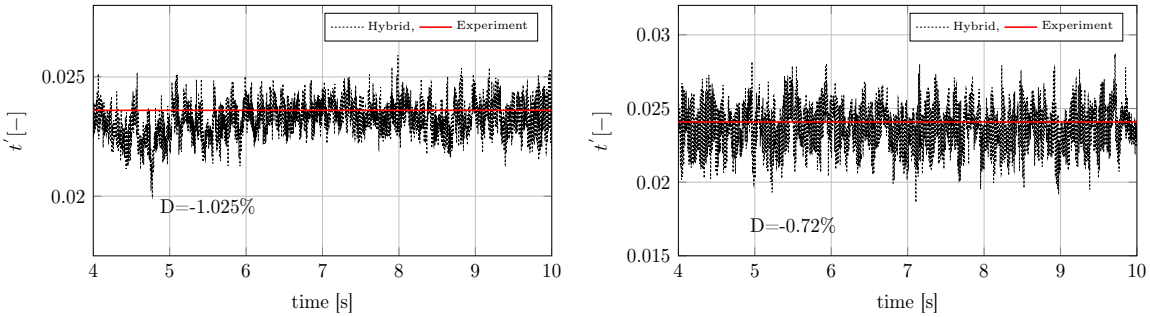

(a) r=0.2, β=12° (b) r=0.6, β=12°

Figure 5: Nondimensional propeller thrust t' for model KVLCC2 at r=0.2, r=0.6 and β=12°.

Table 3: Standard deviations of forces and moments calculated using different approaches under different maneuvering conditions

Z=4	$P'_x/\overline{P_x}\%$	$P'_y/\overline{P_x}\%$	$P'_z/\overline{P_x}\%$	$M'_x/\overline{M_x}\%$	$M'_y/\overline{M_x}\%$	$M'_z/\overline{M_x}\%$	$\Delta P_x/\overline{P_x}\%$
Carlton	6.14±2.2	0.8±0.4	0.85±0.78	4.53±1.95	10.16±6.83	5.57±3.55	16.18±6.19
Wereldsma	7.07±1.41	1.15±1.41	1.14±1.41	4.95±1.41	2.96±1.41	4.04±1.41	20.0±4.0
Shaftdesigner	2.40±1.36	0.50±0.21	0.95±0.43	1.90±1.15	4.31±1.72	6.27±2.08	6.74±3.8
Hybrid, β=0°	3.52	0.44	0.6	2.32	2.93	8.34	23.42
Hybrid, r=0.2, β=6°	5.02	0.46	0.75	2.94	7.91	7.00	34.51
Hybrid, r=0.2, β=12°	4.46	1.20	1.75	2.85	9.05	12.40	32.00
Hybrid, r=0.6, β=12°	6.36	1.85	1.85	4.40	10.72	14.40	45.15

Comparing the CFD data obtained by the hybrid method with the experimental estimations for a ship moving straight forward, we notice that the agreement between both results is quite reasonable. The standard deviations for the forces and moments increase significantly when the ship starts maneuvering (compare, for example, the case $r = 0.2$, β=6°with straight forward motion $r = 0$, $\beta = 0$). This occurs due to more complex vortex

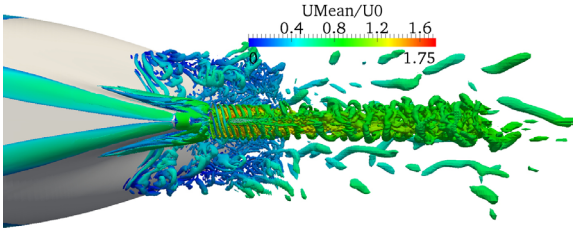

(a) Ship, propeller and rudder, bottom view, $r = 0, \beta = 0^{\circ}$

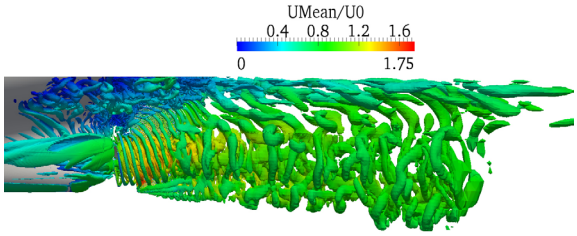

(b) Side view, $r = 0, \beta = 0^{\circ}$

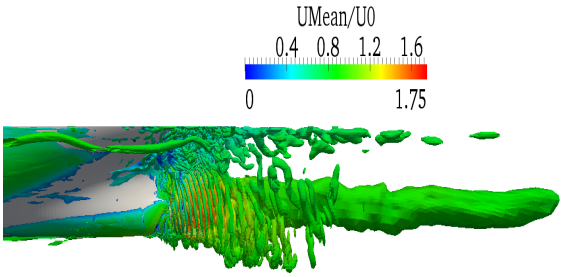

(c) Ship, propeller and rudder, side view, $r = 0.6, \beta = 12^{\circ}$

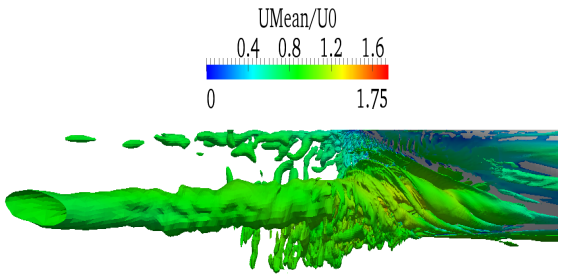

(d) Side view, $r = 0.6, \beta = 12^{\circ}$

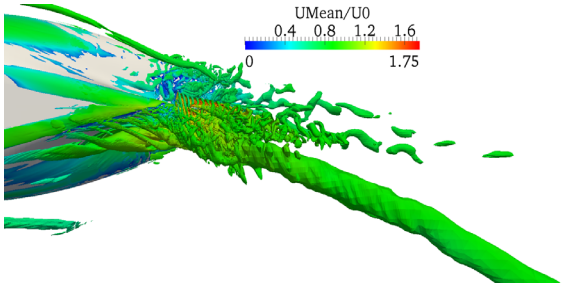

(e) Bottom view, $r = 0.6, \beta = 12^{\circ}$

Figure 6: Vortex structures around the hull with rudder and rotating propeller visualized by $\lambda_2 = -50$ criterion. Computations using the hybrid method at $(r = 0, \beta = 0^{\circ})$ and $(r = 0.6, \beta = 12^{\circ})$.

system and more instabilities in the velocity field behind the ship hull. For instance, the standard deviation for the thrust ratio $P'_x/\overline{P_x}$ reaches 6.5% at $r = 0.6$, β=12°whereas the thrust fluctuations amplitude attains peaks around 42%. As for the standard deviation of transversal forces, it is twice and sometimes more as small as the standard deviation for the thrust. The standard deviation for moments around axis y and z is more than that around x-axis for all studied cases. The main reason for this is the considerable non-uniformity of the wake which causes large moment fluctuations around y and z axis. Back to results for the 5-blade VP1356 propeller, one can reveal the strong difference in thrust oscillations with these for the 4-blade MOERI propeller in case of the ship moving straight forward i.e. without drift angle and yaw rate. In case of the VP1356, the standard

deviation of the thrust related to the mean value is less than 1% whereas it is 3.5% in case of MOERI. Figure. 6 shows vortex structures under maneuver conditions (drift angle and yaw rate) which were obtained using the λ_2-criterion applied to the instantaneous velocity field. As seen the vortex system forming around and behind the ship hull under maneuver conditions is more complicated compared with the case $r = 0$ and $\beta = 0$, which in turn results in the increase of propeller force fluctuations.

6 CONCLUSIONS

The following conclusions can be drawn from the simulations presented above:
• Nonuniformity of the nominal wake increases at maneuvering conditions.
• Influence of the drift angle on the mean thrust is relatively weak. On the contrary the thrust and torque fluctuations increase significantly with β. For instance, the standard deviation (S.D.) of the thrust increases from one to four percent, the S.D. for torque grows from one to three percent when the drift angle changes from zero to 30 degrees.
• Fluctuations of transversal forces and moments gets larger when the drift angle changes from zero to 12 degrees. At larger drift angle $\beta = 30^\circ$ the fluctuations become slightly smaller.
• Force and moment fluctuations becomes sufficiently larger at full maneuvering conditions with drift angle and yaw rate.
• The force and moment fluctuations predicted by IDDES based on SA model are sufficiently larger than these predicted by the Hybrid method. Since the experimental data are not available for maneuvering conditions, at present it is difficult to say about which method has better accuracy. Unrealistic large fluctuations predicted by DMM are due to insufficient resolution of ship boundary layer. For a pure LES simulation it should be much larger.

REFERENCES

[1] Kornev, N., Taranov, A., Shchukin, E., Kleinsorge, L. *Development of hybrid URANS-LES methods for flow simulation in the ship stern area*. Ocean Engineering 38, PP: 1831-1838, (2011).

[2] Abbas, N., Kornev, N. *Study of influence of unsteady wake on the Propeller Performance using the hybrid RANS-LES methods*, Proceedings of Nutt's 2014: 17-th numerical towing tank symposium, Marstrand, Sweden, pp. 9-14, (2014).

[3] Kume, K., Hasegawa, J., Tsukada, Y., Fujisawa, J., Fukasawa, R., and Hinatsu, M. *Measurements of hydrodynamic forces, surface pressure, and wake for obliquely towed tanker model and uncertainty analysis for CFD validation*. Journal of marine science and technology, 11(2), 65-75, (2006).

[4] Ueno, M., Yoshimura, Y., Tsukada, Y., and Miyazaki, H. *Circular motion tests and uncertainty analysis for ship maneuverability.* Journal of marine science and technology, 14(4), 469-484, (2009).

[5] Stern, F., Agdrup, K., Kim, S. Y., Hochbaum, A. C., Rhee, K. P., Quadvlieg, F., and Gorski, J. *Experience from SIMMAN 2008-the first workshop on verification and validation of ship maneuvering simulation methods.* Journal of Ship Research, 55(2), 135-147, (2011).

[6] Xing, T., Shao, J., and Stern, F. *BKW-RS-DES of unsteady vortical flow for KVLCC2 at large drift angles.* In Proc 9th Int Conf on Numerical Ship Hydrodynamics, Ann Arbor, MI (pp. 5-8), (2007).

[7] Shur, M. L., Spalart, P. R., Strelets, M. K., and Travin, A. K. *A hybrid RANS-LES approach with delayed-DES and wall- modelled LES capabilities.* International Journal of Heat and Fluid Flow, 29(6), 1638-1649, (2008).

[8] Batrak, Y.A., Shestopal, V.P., Batrak, R.Y. *Propeller hydrodynamic loads in relation to propulsion shaft alignment and vibration calculations.* Proceedings of Propellers-Shafting 2012 Symposium, 10.1-10.14, (2012).